COMPARISON OF FLUX DATA DEDUCED FROM OBSERVED IMPACTS ON LDEF WITH PREDICTIONS FROM METEOROID AND DEBRIS MODELS

D.H. Niblett, S. Mullen, M.J. Neish and J.A.M. McDonnell

Unit for Space Sciences, University of Kent at Canterbury, Canterbury, Kent CT2 7NR, UK.

ABSTRACT

The retrieval of the Long Duration Exposure Facility (LDEF) in January 1990 provided a vast amount of information concerning interplanetary meteoroids and space debris particles. An earlier survey of the flux data derived from impacts on LDEF experimental surfaces pointing in different directions and on the LDEF spacecraft itself has been updated by the incorporation of more recent observations. These include more detailed examination of the A0023 Micro Abrasion Package (MAP) foils and the S0002 Space Debris Impact Experiment (SDIE), together with data from the A0138 FRECOPA experiment, measurements of craters in aluminium clamps and information on the Meteoroid and Debris Special Investigation Group database. Flux data and ratios significant to modelling are calculated for particles able to penetrate equivalent thicknesses of aluminium ranging from 1 μm to 680 μm. These are compared with predictions of the number of penetrations of meteoroids and space debris particles through different LDEF faces calculated by Drolshagen using the ESABASE analysis tool.

1. INTRODUCTION

The Long Duration Exposure Facility (LDEF), which orbited the Earth at a mean altitude of 458 km from 1984 to 1990, carried several experiments specifically designed to measure the flux of micrometeoroids and debris particles striking the different faces of the spacecraft. In addition, the Meteoroid and Debris Special Investigation Group (MD-SIG) examined the whole spacecraft after recovery and documented all the large craters on it. This MD-SIG documentation formed the basis of an impact database which has since been extended to incorporate smaller craters and penetration holes.

The LDEF spacecraft was stabilized such that its long axis always pointed towards the centre of the Earth and its twelve peripheral surfaces always pointed at fixed angles relative to the direction of its orbital motion (Ref. 1). The various experiments were located on a number of these surfaces and the experimenters have produced plots of flux against either crater diameter or foil penetration thickness for each direction. It is desirable to try to arrive at agreed values of the flux for each direction as a function of particle size, taking into account all the available data. There are, however, a number of factors which make this difficult. Firstly, it has been observed, in the Interplanetary Dust Experiment (Ref. 2), that the impact rate was very strongly time-dependent, with evidence that LDEF encountered the same cloud of orbital particles on many successive orbits; thus only experiments which operated for the whole mission can be expected to record comparable fluxes. Secondly, some data relate to crater diameters and others to foil perforations. The relation between these data sets depends on the properties of the impacting particle and of the target material. Because the majority of the measured impacts were in aluminium surfaces, the problem of different target materials can be avoided by restricting our attention to aluminium. However, since the impacts are produced by a combination of natural particles and man-made debris, it is inevitable that a range of impactor properties will occur. It is, moreover, important to try to distinguish between the contributions of interplanetary and orbital particles to the total flux observed. A key to this is provided by comparing the flux observed on different faces of LDEF, because access to the different faces is in general different for orbital and interplanetary particles. An earlier paper (Ref. 3) discussed some key ratios of fluxes in different directions for particles of different sizes. Considerably more data are now available and the purpose of this paper is to present updated values of these flux ratios and to compare them with predictions based on modelling of interplanetary particles and orbital debris.

2. SMOOTHED FLUX DATA

The impact data are first presented in the form of the flux (in $m^{-2}\ s^{-1}$) of particles which would perforate an aluminium foil of a certain thickness f_{max} (in μm) on a particular face of LDEF.

Figure 1 shows such flux curves for LDEF's leading face (Row 9), trailing face (Row 3) and Space-facing surface. The only data which actually relate to aluminium foil perforations are for the A0023 Micro Abrasion Package (MAP) (Ref. 4), for foil thicknesses in the range between 5 μm and 31 μm. The other portions of the flux curves are based on measurements of the diameter D_C of craters in the surfaces. As indicated earlier, the relation between D_C and f_{max} depends on

the velocity, density and other properties of the impacting particles (Ref. 5). For the present paper, we have assumed that a particle which made a crater of diameter D_c in a semi-infinite aluminium surface would have just perforated an aluminium foil of thickness $f_{max} = 0.78\ D_c$ for craters larger than 30 μm, or $f_{max} = 0.93\ D_c$ for smaller craters. The data for foil thicknesses less than 5 μm were mainly obtained by measuring crater diameters in the MAP foils. In the case of Row 3, the data from the A0138 French Cooperative Payload (FRECOPA) (Ref. 6) were also used in this size range. The data for the upper end of the size range (f_{max} > 390 μm) were obtained from the S0002 Space Debris Impact Experiment (SDIE) (Ref. 7). For the Row 3 and Row 9 plots, the fluxes in the intermediate size range (30 - 390 μm) were derived from measurements of craters on the aluminium intercostals of the LDEF framework, as recorded in the MD-SIG database (Ref. 8). In the case of the Space face, for which the only MAP aluminium foil was 5 μm thick, the flux curve was determined from the diameters of craters and of perforation holes (Ref. 5) in this foil and also from the diameters of craters in the aluminium clamps (Ref. 9) which fastened the MAP experiment tray to the framework, as well as the SDIE results for large craters in aluminium. In all cases, the flux curves plotted are smoothed curves chosen, with the aid of a computer smoothing routine, to give a consistent best fit through the experimental data; the actual experimental points are omitted from the figure here, but can be found in Ref. 5.

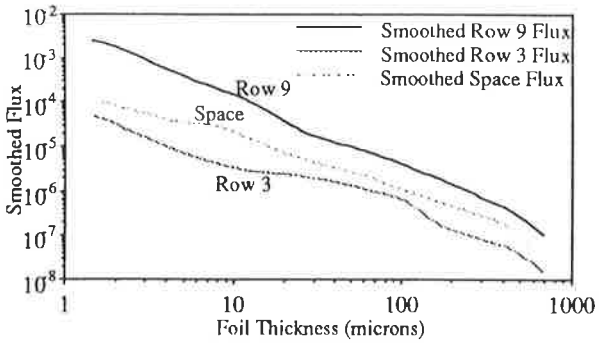

Figure 1. Smoothed cumulative flux (in $m^{-2}\ s^{-1}$) versus equivalent aluminium foil perforation thickness f_{max} (in μm) for surfaces on Row 3, Row 9 and the Space-pointing face of LDEF.

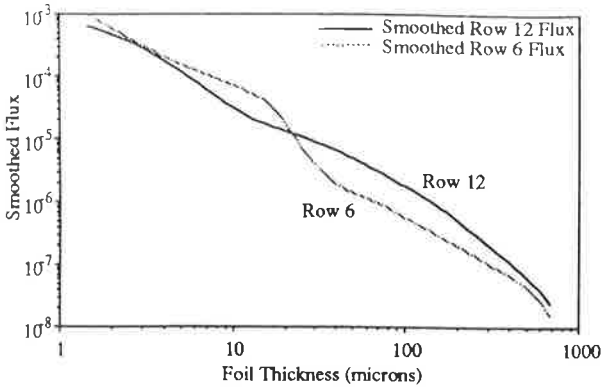

Figure 2. Smoothed cumulative flux (in $m^{-2}\ s^{-1}$) versus equivalent aluminium foil perforation thickness f_{max} (in μm) for surfaces on Row 6 and Row 12 of LDEF.

Figure 2 shows flux curves for the side faces of LDEF, Row 6 (South) and Row 12 (North). These were obtained in a similar manner, using the MAP, intercostals and SDIE data in the appropriate size ranges. We note that these two flux curves cross over at a foil thickness of about 22 μm.

3. CORRECTION FOR LDEF OFFSET

The direction of the LDEF velocity vector was not exactly normal to Row 9: it was displaced by approximately 8 degrees towards Row 10. Thus Row 9 was not facing East exactly and it would be very useful to try to deduce the fluxes which would have been encountered by the East, West, North and South faces if LDEF had been orientated so that a face (East) was exactly normal to the velocity vector.

One way to do this is to plot the flux values for Rows 3, 6, 9 and 12, for any given value of f_{max}, against the angle θ from Row 9. Figure 3 shows such a plot for the perforations of the MAP 5 μm aluminium foil. The curve chosen to represent the angular flux distribution is of the form

$$\text{Flux} = A + B\cos(\theta + \phi) + C\cos 2(\theta + \phi) \qquad (1)$$

where the four parameters A, B, C and φ are chosen so that the curve passes through the four flux points. This curve is then used to find the flux values at angles θ of -172, -82, 8 and 98 degrees (i.e. displaced by 8 degrees from Rows 3, 6, 9 and 12) to give the corrected flux values for the true West, South, East and North directions respectively. This correction makes little change for the West and East faces, as the flux curve is fairly flat near the minimum and maximum, but has a larger effect for the South and North faces because the gradient is steep in these regions.

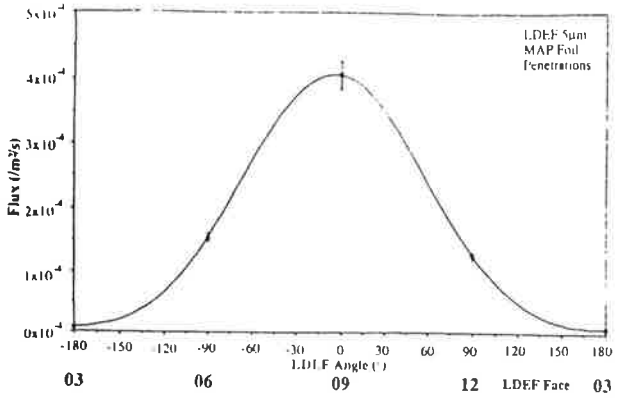

Figure 3. Angular dependence (relative to Row 9 of LDEF) of the perforations of the MAP 5 μm aluminium foil.

The above procedure was carried out for eighty values of f_{max} and the corrected flux curves are shown in Figures 4 and 5. As indicated above, the corrected East and West fluxes (Fig. 4) show little change from those for Rows 9 and 3 (Fig. 1). Larger changes occur on Figure 5, the South flux values being increased and the North values reduced so that the intersection of the flux curves now occurs at a foil thickness of 24 μm.

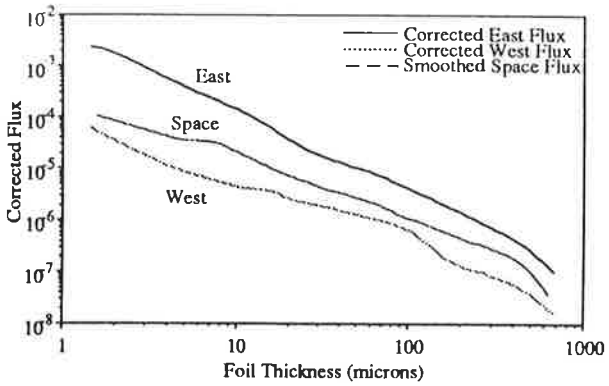

Figure 4. Flux distributions which would have occurred on the East, West and Space faces of LDEF if the East face had been normal to the velocity vector.

4. LDEF FLUX RATIOS

The ratios of the fluxes in certain directions are critical factors in the comparison of the LDEF experimental data with predictions from models of the natural and debris particle populations. Flux ratios can be evaluated for either the actual LDEF faces or the true East, West, North and South directions using the corrected flux values deduced in Section 3 above.

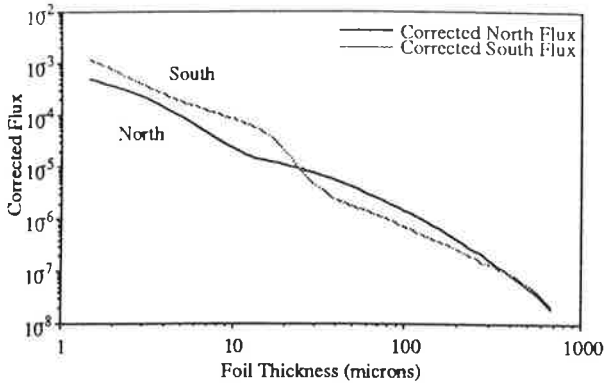

Figure 5. Flux distributions which would have occurred on the North and South faces of LDEF if the East face had been normal to the velocity vector.

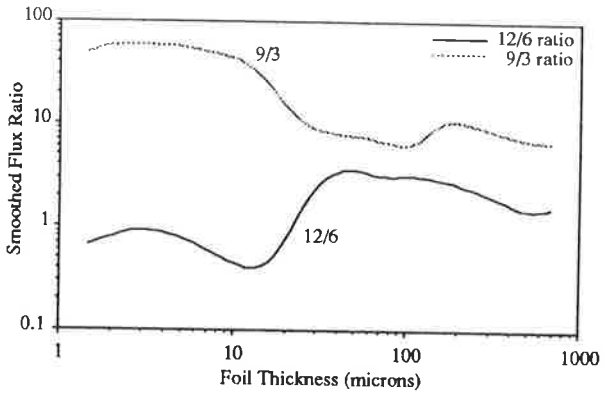

Figure 6. LDEF flux ratios for Row 9/Row 3 and Row 12/Row 6, obtained from the smoothed fluxes shown in Figures 1 and 2, plotted against the equivalent aluminium foil perforation thickness f_{max} (in μm).

Figure 6 shows the ratio of the flux on Row 9 to that on Row 3 and also the ratio of the flux on Row 12 to that on Row 6, both plotted against the equivalent aluminium foil perforation thickness f_{max}.

The 9/3 ratio is in the range between 6 and 11 for the larger particles capable of penetrating more than 24 μm of aluminium, but increases to about 50 for foil thicknesses below about 10 μm. Drolshagen (Ref. 10) has used the ESABASE analysis tool, based on the latest meteoroid and debris flux models (Refs. 11, 12), to calculate the numbers of impacts from meteoroids and space debris which would penetrate through 5 μm or 180 μm aluminium foils on the various faces of LDEF. We can use his calculations to determine predicted values for the 9/3 flux ratio for these foil thicknesses and compare them with the experimental values shown in Figure 6 (Table 1).

Table 1 shows that the predicted values of the 9/3 flux ratio are much larger than those observed, particularly

at f_{max} = 5 μm. This difference (at 5 μm) arises mainly because the model predicts a much higher flux on Row 9 than was observed experimentally. As the particles penetrating the 5 μm foil on Row 9 are predicted by ESABASE to be 97% debris, we see that the Kessler model utilised in ESABASE must over-estimate the debris contribution in this size range. However, the ESABASE prediction at 5 μm for meteoroids only (also shown in Table 1) gives a 9/3 ratio considerably lower than the observed value, showing that the majority of the perforations of this foil must have been caused by orbital particles. On the other hand, the high predicted value of the 9/3 ratio at f_{max} = 180 μm arises because the ESABASE model predicts a much smaller flux on Row 3 than was observed. The model is based on the approximation that all debris is moving in circular orbits and therefore produces very few impacts on Row 3. However, there is chemical evidence from the A0187-1 Chemistry of Micrometeoroids Experiment (Ref. 13) for debris impacts on Row 3, showing that debris in elliptical orbits must contribute to the flux on this face. Debris in elliptical orbits would reduce the predicted 9/3 ratio, but not sufficiently to account for all the discrepancy. The ratio predicted for meteoroids alone is considerably larger than that observed at this size, but it is to be noted that this ratio depends strongly on the meteoroid velocity distribution used (Ref. 14).

f_{max} (μm)	Observed 9/3	Predicted 9/3	Predicted 9/3 meteoroids
5	56	546	15
180	10.5	38	26

Table 1. Comparison of the observed and predicted values of the LDEF Row 9/Row 3 flux ratio.

The 12/6 flux ratio is found to be greater than unity for foil thicknesses greater than 22 μm and less than unity for smaller particles. The observations for f_{max} values of 5 μm and 180 μm are compared with the ESABASE predictions in Table 2.

f_{max} (μm)	Observed 12/6	Predicted 12/6	Predicted 12/6 meteoroids
5	0.77	2.5	1.4
180	2.7	1.8	1.5

Table 2. Comparison of the observed and predicted values of the LDEF Row 12/Row 6 flux ratio.

We note that the ESABASE predictions, even for meteoroids alone, give 12/6 ratios greater than unity because of the offset of the LDEF velocity vector towards the North. However, the observed ratio at f_{max} = 5 μm is less than unity. More than 95% of the perforations of the 5 μm foils on Rows 6 and 12 are predicted to be caused by debris and again the predicted flux values on both these surfaces are considerably higher than those observed.

The upper graph in Figure 7 shows the ratio of the flux on the Space face to that on Row 3, which is particularly significant because both of these faces were impacted mainly by extraterrestrial particles. Values of this Sp/3 ratio are seen to range between 1.7 (for f_{max} near 100 μm) and 6.9 (for f_{max} near 8 μm). The fact that this flux ratio appears to fall below 2 for the range of f_{max} between about 60 μm and 120 μm implies that these particles, although mainly interplanetary, must include some debris in elliptical orbits.

The comparison with the ESABASE predictions (Table 3) shows that the observed Sp/3 ratio is lower than that predicted for both particle sizes. This can again be partially attributed to the neglect of the debris in elliptical orbits; these would increase the flux on Row 3, but there remains some disagreement between predictions and observations for meteoroids on Row 3.

The lower graph in Figure 7 shows the ratio of the flux on the Space face to the average of the fluxes on Rows 6 and 12. This Sp/6,12 ratio increases fairly steadily with size from 0.14 to about 2. The observed values are compared with ESABASE predictions in Table 4.

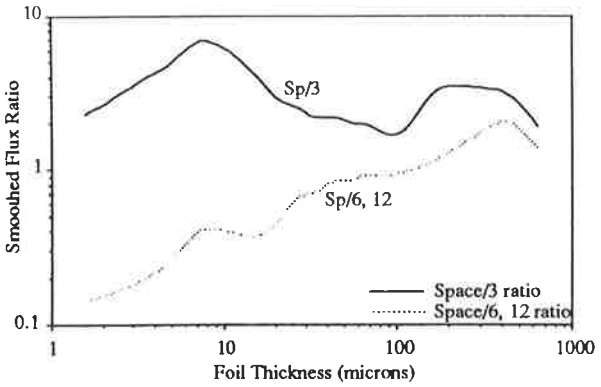

Figure 7. Ratios of the flux on the Space face of LDEF to the flux on Row 3 and to the average of the fluxes on Rows 6 and 12, obtained from the smoothed fluxes shown in Figures 1 and 2.

f_{max} (μm)	Observed Sp/3	Predicted Sp/3	Predicted Sp/3 meteoroids
5	5.0	8.7	8.7
180	3.4	11.2	11.2

Table 3. Comparison of the observed and predicted values of the LDEF Space/Row 3 flux ratio.

f_{max} (μm)	Observed Sp/6,12	Predicted Sp/6,12	Predicted Sp/6,12 meteoroids
5	0.26	0.045	1.33
180	1.2	0.87	1.26

Table 4. Comparison of the observed and predicted values of the ratio of the Space flux to the average of the fluxes on Rows 6 and 12.

The ESABASE calculations show that the Sp/6,12 ratio should be about 1.3 for meteoroids only and is insensitive to the particle size. For debris in circular orbits this ratio should of course be zero, since these particles are unable to strike the Space face. Hence this ratio is very significant in determining the ratio of interplanetary to orbital particles at any given size. It shows that interplanetary particles must predominate at f_{max} = 180 μm. However, since it falls below about 0.65 for f_{max} values below about 26 μm, there must be more orbital particles than meteoroids at these smaller sizes. The very low predicted ratio at f_{max} = 5 μm again follows from the apparent over-estimate of the debris contribution in this size range.

We can also evaluate these flux ratios for the true East, West, North and South directions using the flux values as corrected for the offset of the LDEF velocity vector. Figure 8 shows the corrected East/West and North/South flux ratios. The E/W ratio has a value in the region of 10 for the larger particles, which is in reasonable agreement with modelling by Zook (Ref. 14) for meteoroids, provided that the Dohnanyi velocity distribution (Ref. 15) is used. The increased values of the ratio for f_{max} less than about 20 μm are due to the predominance of orbital particles which are unlikely to strike the trailing face. These orbital particles are not necessarily all debris; McDonnell and Ratcliff (Ref. 16) have argued the case for an orbital component of natural particulates. There is some evidence for a decrease in the E/W ratio for f_{max} values below 2 μm. The Interplanetary Dust Experiment (Ref. 2), using semiconductor detectors for the first year only of the mission, found this ratio to be in the region of 10 for very small particles.

The corrected N/S ratio (Fig. 8) is particularly significant because a random distribution of particle trajectories would of course imply that this ratio should be unity. It is found to be near to unity for the largest particles, but rises to about 2 for a range of f_{max} between about 30 μm and 150 μm. It then falls to unity at f_{max} = 24 μm and is below 0.6 for all values of f_{max} less then 20 μm. Thus there is evidence for asymmetry of both the orbital and the interplanetary particles. For the small particle region, where the E/W and Sp/6,12 ratios have shown that the orbital particles must predominate, there is a bias in favour of impacts on the South face. Evidence for an asymmetric population of space debris is considered in a separate paper (Ref. 17). For the larger particles, which are shown by the Sp/6,12 ratio to be mainly interplanetary, there is a bias in favour of impacts on the North face. This implies an excess of meteoroids in descending nodes at the time of the LDEF mission, which is being investigated further (Ref. 18).

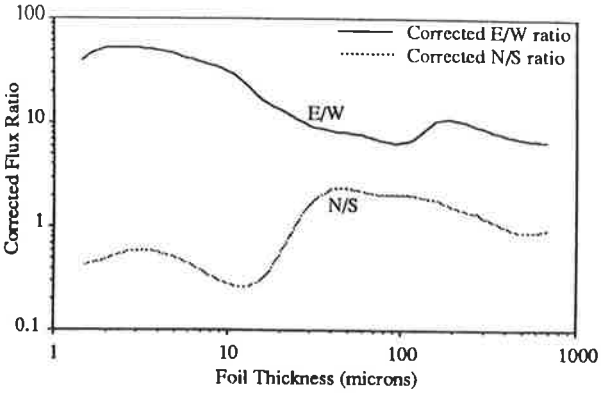

Figure 8. LDEF flux ratios for East/West and North/South, obtained from the fluxes shown in Figures 4 and 5 which would have occurred if the East face had bee normal to the velocity vector.

The correction for the LDEF offset has very little effect on the ratios shown in Figure 7, so the corrected Sp/W and Sp/N,S flux ratios are not shown.

5. CONCLUSIONS

The experimental data from LDEF reviewed here provides a basis for comparison via ESABASE or other analytical techniques with current models of meteoroid and debris fluxes. Comparison of the observed LDEF flux ratios with ESABASE predictions shows clearly that orbital particles must predominate for the smaller size range, capable of perforating up to about 20 μm of aluminium, and that interplanetary particles must predominate for the larger size range, with f_{max} greater than about 30 μm. It also provides evidence for an appreciable amount of debris in elliptical orbits, in support of other findings (Refs. 13, 19, 20). This comparison with Drolshagen's ESABASE predictions (Ref. 10) implies that the current debris models over-estimate the debris population in the micron size range. However, this appears to conflict with similar comparisons made by Mandeville and Berthoud (Ref. 21), who report good agreement between the observed and computed fluxes on LDEF's leading and trailing faces. Further comparisons will be made for different particle sizes to try to resolve this, and the debris model should be refined if necessary to obtain better agreement with the observations.

The smoothed flux curves will be improved by incorporating data from more LDEF impact surfaces and by refining the relation between crater diameter

and equivalent foil perforation thickness. The flux curves for the larger particles can also be improved by making use of data from more than four of the peripheral faces. For example, the intercostals and longerons of the LDEF framework together provide data for 24 different peripheral directions, thus permitting a better determination of the angular distribution function of the flux and hence of the corrected fluxes for the East, West, North and South directions.

6. ACKNOWLEDGEMENTS

The authors acknowledge the support of the UK Science and Engineering Research Council and the European Social Fund.

7. REFERENCES

1. O'Neal, R.L. and Lightner, E.B., Long Duration Exposure Facility - A General Overview, *LDEF - 69 Months in Space, First Post-Retrieval Symposium*, NASA CP-3134, 3, 1991.

2. Mulholland, J.D. et al., IDE Spatio-Temporal Impact Fluxes and High Time- Resolution Studies of Multi-Impact Events and Long Lived Debris Clouds, *LDEF - 69 Months in Space, First Post-Retrieval Symposium*, NASA CP-3134, 517, 1991.

3. Niblett, D.H., Survey of Flux Data Derived from Impacts on LDEF Surfaces, *Hypervelocity Impacts in Space*, Editor J.A.M. McDonnell, University of Kent at Canterbury, 227, 1992.

4. McDonnell, J.A.M. et al., First Results of Particulate Impacts and Foil Perforations on LDEF, *Advances in Space Research*, Vol. 11, No. 12, 109, 1991.

5. McDonnell, J.A.M. et al., The Near Earth Space Impact Environment - An LDEF Overview, *Proceedings of IAF/COSPAR World Congress*, Editor W. Flury, Pergamon, 1993.

6. Mandeville, J.C. and Borg, J., Study of Cosmic Dust Particles On Board LDEF, The FRECOPA Experiments A0138-1 and A0138-2, *LDEF - 69 Months in Space, First Post-Retrieval Symposium*, NASA CP-3134, 419, 1991.

7. Humes, D.H., Large Craters on the Meteoroid and Space Debris Impact Experiment, *LDEF - 69 Months in Space, First Post-Retrieval Symposium*, NASA CP-3134, 399, 1991.

8. Meteoroid and Debris Special Investigation Group, LDEF Database, *NASA JSC Houston*.

9. Newman, P.J., Comparison of the Micrometeoroid Environment as Measured by Thick and Thin Targets from the East Face of the Long Duration Exposure Facility, *Hypervelocity Impacts in Space*, Editor J.A.M. McDonnell, University of Kent at Canterbury, 223, 1992.

10. Drolshagen, G., Meteoroid/Debris Impact Analysis. Application to LDEF, Eureca and Columbus, *First European Conference on Space Debris*, Darmstadt, 1993.

11. Grun, E. et al., Collisional Balance of the Meteoritic Complex, *Icarus*, Vol. 62, 244, 1985.

12. Kessler, D.J. et al., Orbital Debris Environment for Spacrcraft Designed to Operate in Low Earth Orbit, *NASA TM-100-471*, 1989.

13. Bernhard, R.P. et al., Preliminary Analysis of LDEF Instrument A0187-1, *LDEF Second Post-Retrieval Symposium*, San Diego, 1992.

14. Zook, H.A., Deriving the Velocity Distribution of Meteoroids from the Measured Meteoroid Impact Directionality on the Various LDEF Surfaces, *LDEF - 69 Months in Space, First Post-Retrieval Symposium*, NASA CP-3134, 569, 1991.

15. Dohnanyi, J.S., Model Distribution of Photographic Meteors, *Bellcomm TR-66-340-1*, Bellcomm Inc., 1966.

16. McDonnell, J.A.M. and Ratcliff, P.R., The Geocentric Particulate Distribution: Cometary, Asteroidal or Space Debris? *Asteroids, Comets Meteors*, Proceedings of the International Conference, Flagstaff, Arizona, Lunar and Planetary Institute, Houston, 407, 1992.

17. McDonnell, J.A.M., The LEO Particulate Environment: LDEF's 5.75 Year Perspective on Orbital Space Debris and Meteoroids, *First European Conference on Space Debris*, Darmstadt, 1993.

18. McBride, N., *Personal communication.*

19. Flury, W. et al., Space Debris in Elliptical Orbits, *18th Symposium in Space Technology and Science*, Kagoshima, Japan, 1992.

20. Kessler, D.J., Collision Probability at Low Altitudes Resulting from Elliptical Orbits, *Advances in Space Research*, Vol. 10, No. 3-4, 393, 1990.

21. Mandeville, J.C. and Berthoud, L., Orbital Debris and Meteoroids: Results from Retrieved Space Experiments, *First European Conference on Space Debris*, Darmstadt, 1993.